An Automatic Detection Software for Differential Reflection Spectroscopy

Seniha Esen Yuksel[a, b], Thierry Dubroca[a], Rolf E. Hummel[a], Paul D. Gader[b]

[a]Department of Materials Science and Engineering, University of Florida, Gainesville, FL, USA
[b]Department of Computer and Information Science and Engineering, University of Florida, Gainesville, FL, USA

ABSTRACT

Recent terrorist attacks have sprung a need for a large scale explosive detector. Our group has developed differential reflection spectroscopy which can detect explosive residue on surfaces such as parcel, cargo and luggage. In short, broad band ultra-violet and visible light is shone onto a material (such as a parcel) moving on a conveyor belt. Upon reflection off the surface, the light intensity is recorded with a spectrograph (spectrometer in combination with a CCD camera). This reflected light intensity is then subtracted and normalized with the next data point collected, resulting in differential reflection spectra in the 200-500 nm range. Explosives show spectral finger-prints at specific wavelengths, for example, the spectrum of 2,4,6, trinitrotoluene (TNT) shows an absorption edge at 420 nm. Additionally, we have developed an automated software which detects the characteristic features of explosives. One of the biggest challenges for the algorithm is to reach a practical limit of detection. In this study, we introduce our automatic detection software which is a combination of principal component analysis and support vector machines. Finally we present the sensitivity and selectivity response of our algorithm as a function of the amount of explosive detected on a given surface.

Keywords: Explosive detection, support vector machines, PCA, hyperspectral data, differential reflectometry, spectroscopy

1. INTRODUCTION

In the aftermath of 9/11 and the attempted shoe bombing of the American Airlines Flight in December 2001, there has been a dramatic increase in the explosive detection research to decrease the threats at the airports, parcel screening checkpoints, as well as at parks, roadsides and public transports.[1–6] Transportation Security Administration (TSA) screens over 625 million passengers a year through 2200 security checkpoint lanes; cargo industry handles 43 million metric tons of freight annually, and the United States Postal Service delivers over 80 billion pieces of first-class mail. Given these large numbers, what we need are fast and efficient systems that can scan large volumes of luggage and parcel, do not need an operator, are sensitive to trace amounts and that are not restricted to any chemical groups such as nitrogen. With such systems, it should be possible to scan every bag and every parcel that goes through a screening point without infringing on individual rights nor disrupting the flow of goods or people.

At the University of Florida, we have developed the differential reflectometer (DR) (also known as the differential reflection spectrometer) that detects explosive materials on surfaces such as luggage, parcels, and mail.[7–17] The schematic of the system is shown in Fig. 1(a), where the detector is placed at the top of the conveyor belt. The detector is composed of the components shown in Fig. 1(b), where a broad band ultra violet (UV)-visible light source is shone onto a conveyor belt, and the reflected light is collected with a spectrometer and recorded with a CCD camera. The spectrometer separates the broad band light into the wavelengths between 200nm and 6002nm, and the spectra collected from each pixel of the probed surface is the reflectivity at that pixel, denoted by R. As the luggage moves on the conveyor belt, two consecutive measurements are recorded, which are denoted by R_1 and R_2, and differential reflectogram (DR) is computed as the normalized difference in reflectivity, given by

$$\Delta R/\bar{R} = 2(R_2 - R_1)/(R_1 + R_2).$$

Algorithms and Technologies for Multispectral, Hyperspectral, and Ultraspectral Imagery XVIII, edited by Sylvia S. Shen, Paul E. Lewis, Proc. of SPIE Vol. 8390, 83900B · © 2012 SPIE
CCC code: 0277-786X/12/$18 · doi: 10.1117/12.919431

Downloaded From: http://proceedings.spiedigitallibrary.org/ on 12/25/2016 Terms of Use: http://spiedigitallibrary.org/ss/termsofuse.aspx

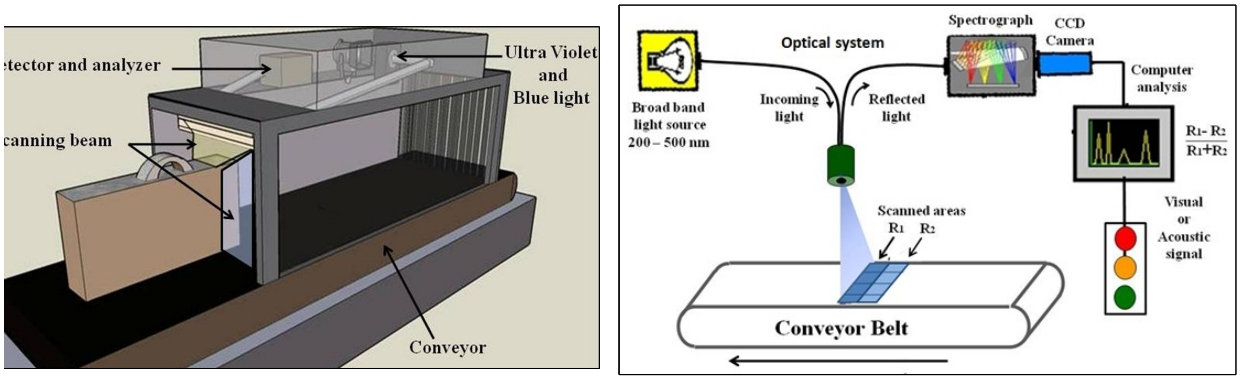

(a) (b)

Figure 1. Schematic of the system. (a) The explosive scanner is placed at the top, and scans each luggage as they pass on the conveyor belt. (b) The optical plot of the DR system. A a broad band ultra violet (UV)-visible light source is shone onto a conveyor belt, and the reflected light is collected with a spectrometer and recorded with a CCD camera.

.

With DR, explosives show signature patterns at specific wavelengths. For example, spectra of TNT shows a sudden decrease at 420nm as shown in Fig. 2. In this figure, several other visually confusers are displayed, such as flour, Splenda and salt. Each spectra is obtained from a single pixel, and several spectra of the same color are obtained from different pixels of the same substance. This shows the reproducibility of the DR system.

2. SOFTWARE

About 2000 TNT spectra and 23000 non-TNT spectra were collected with various amounts of TNT placed on handbags, clothes and boards as the background. In these data acquisitions, it was observed that the height of the TNT shoulder is determined by the amount of TNT in a given pixel. This aspect is shown in Fig. 3 where the log-magnitude of the spectra was plotted as a histogram. Consider a data set of observations $\{\mathbf{a}_n\}$ where $n = 1, ..., N$ indicates the data index, and $\mathbf{a}_n$ is of dimensionality D, denoted as $\mathbf{a} = [a_1, ..., a_D]$. The log-magnitude of a TNT spectrum is computed as $\log \sqrt{\sum_{d=1}^{D} (a_d)^2}$. When we display the number of TNT spectra in a given bin of similar log-magnitudes, i.e. the histogram, it can be seen that the number of samples can roughly be divided into four as shown in Fig. 3. In the rest of this paper, we consider the samples on the very left side as low magnitude, the samples in the middle as medium magnitude, and the samples on the right hand side as the high magnitudes. Four samples from each of these bins are displayed in Fig.4. We compute the signal to noise ratio (SNR) of each TNT spectrum as the amplitude of the noise on the right hand side of the spectrum multiplied by four and divided by the height at the 420nm shoulder. These SNR rates correspond to amounts of roughly 400 ng, 2 μg, and 100 μg in Fig.4(b-d).

For classification of each spectrum into TNT vs non-TNT classes, each spectrum was filtered with a median and an averaging filter, and cropped to be between the wavelengths of 350nm-450nm. To further reduce the dimensionality of the data, Principal Component Analysis (PCA) was applied, and each spectrum was projected onto the most important 5 eigenvectors. This new (projected) data will be denoted as $\mathbf{x}$. The details of PCA were given in.[16] Then, Support Vector Machine[18] classifiers were trained that maximize the margin among the two classes.[19] For a feature-space transformation $\phi(\mathbf{x}_n)$ that is related to a Mercer Kernel, SVM finds a hyper-plane $\mathbf{w}^T \phi(\mathbf{x}) + b = 0$ in the kernel space, that has the largest distance to the nearest training data points of any class. To find the parameters $\mathbf{w}$ and b of the hyperplane, SVM solves a constrained optimization problem given as:

E-mail: seyuksel@cise.ufl.edu, dubroca@ufl.edu, rhumm@mse.ufl.edu, pgader@cise.ufl.edu

Downloaded From: http://proceedings.spiedigitallibrary.org/ on 12/25/2016 Terms of Use: http://spiedigitallibrary.org/ss/termsofuse.aspx

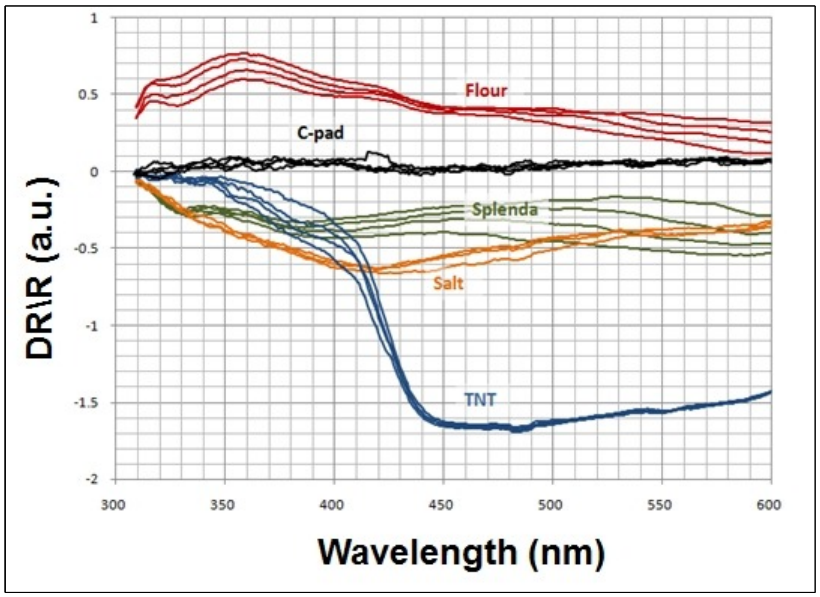

Figure 2. TNT versus the visual confusers. TNT shows a sudden decrease at 420nm which we refer to as TNT's signature. This signature is different from the visual confusers such as flour, Splenda and salt as shown. Here, the C-pad refers to the carbon pad, which was used as the background for all of these substances. Each line represents a spectrum obtained from one pixel. Several spectrum of the same color show the reproducibility of the DR system, as each line was obtained from a different pixel of the same substance.

$$\min_{\mathbf{w},b} \max_{\boldsymbol{\alpha}} \{\frac{1}{2}\|\mathbf{w}\|^2 - \sum_{n=1}^{N} \alpha_n [y_n(\mathbf{w}^T \phi(\mathbf{x}_n) + b) - 1]\}$$

where $\boldsymbol{\alpha} = (\alpha_1, ..., \alpha_N)^T$ are Lagrange multipliers, and y_n is either 1 or 1 such that $\{y_n \in \{-1, 1\}\}_{n=1}^N$, indicating the class to which the point $\mathbf{x}_n$ belongs.

In order to classify new data points using the trained model, we evaluate the sign of $y(\mathbf{x})$, defined by:

$$y(\mathbf{x}) = \mathbf{w}^T \phi(\mathbf{x}) + b \quad .$$

A dataset of 25000 spectra composed of TNT and non-TNT spectra were used, and the SVM classifiers were tested and trained using 2-fold cross validation with a polynomial kernel ϕ. As previously stated, TNT spectra has lower magnitudes for lower amounts of TNT, as shown in Fig. 3. Therefore, training a single SVM classifier does not generalize well to all of the data. This aspect is shown in Fig. 5 where an SVM was trained on TNT spectra with high magnitudes, and tested on TNT with high, medium and low magnitudes. The receiver operating characteristic (ROC) curves of this classifier indicates that the detection of small amounts of TNT is not reasonable with this classifier. To solve this problem, we trained three classifiers that better capture the properties of TNT in each bin. Hence, on the transformed space, three SVM classifiers were trained, one for low magnitude TNT spectra, and one for medium, and one for high magnitude TNT spectra. These results are displayed in Fig. 6 where we are able to get good detection rates for every magnitude of TNT.

Downloaded From: http://proceedings.spiedigitallibrary.org/ on 12/25/2016 Terms of Use: http://spiedigitallibrary.org/ss/termsofuse.aspx

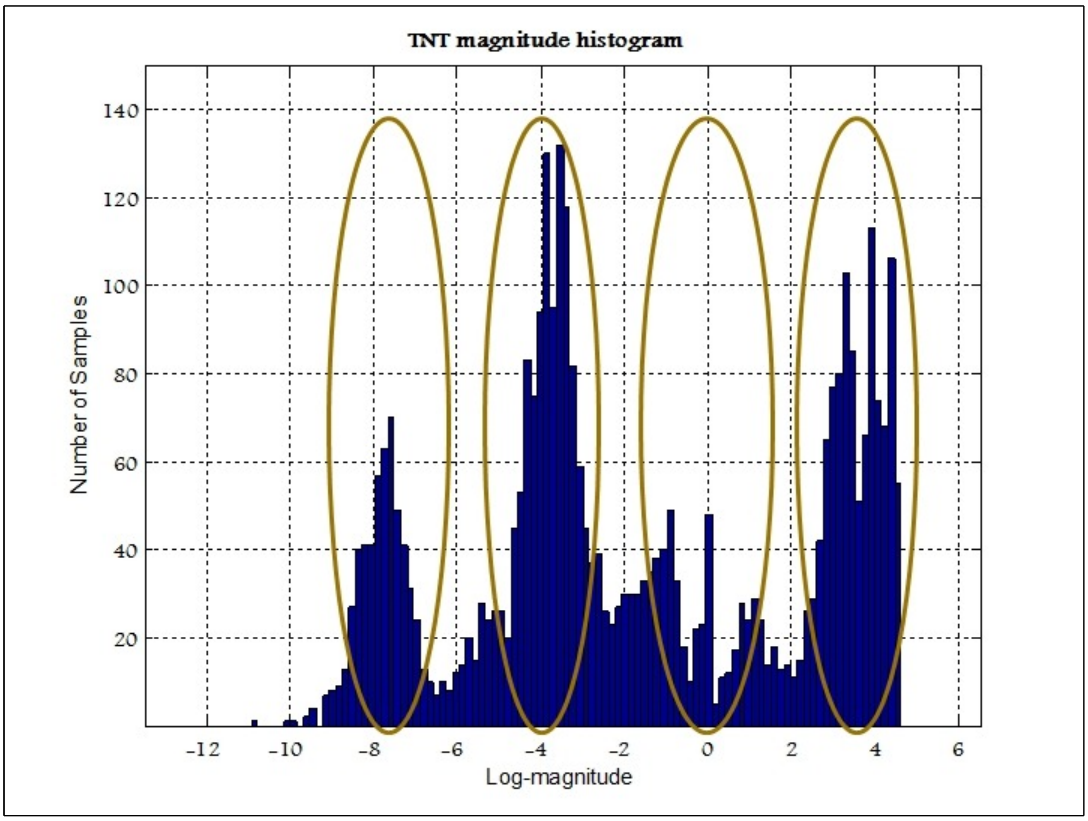

Figure 3. The software.

3. CONCLUSION

In this study, we have described the differential reflectometry system with both its hardware and software. For the DR software, we divided the TNT spectra into low, medium and high magnitudes and trained SVM classifiers for each of these magnitudes. In doing so, we have increased the classification rates to levels that were not possible by training a single SVM classifier. Still, there is room for improvement at the low magnitude levels, and our future work is on employing end-member detection techniques to better identify the explosive signatures. With the design of classifiers that can identify these signatures, it should be possible to eventually check every piece of luggage, cargo, and passengers that boards an aircraft.

REFERENCES

[1] Janni, J., Gilbert, B., Field, R., and Steinfeld, J., "Infrared absorption of explosive molecules," *Spectrochim Acta A* **53**, 1375–1381 (1997).

[2] Muralidharan, G., Wig, A., Pinnaduwage, L. A., Hedden, D., Thundat, T., and Lareau, R. T., "Adsorption-desorption characteristics of explosive vapors investigated with microcantilevers," *Ultramicroscopy* **97**(1–4), 433 – 439 (2003).

[3] Jr., F. C. D. L., Harmon, R. S., McNesby, K. L., Jr., R. J. W., and Miziolek, A. W., "Laser-induced breakdown spectroscopy analysis of energetic materials," *Applied Optics* **42**(30), 6148–6152 (2003).

[4] Manolakis, D., Marden, D., and Shaw, G. A., "Hyperspectral image processing for automatic target detection applications," *Lincoln Laboratory Journal* **14**(1) (2003).

Downloaded From: http://proceedings.spiedigitallibrary.org/ on 12/25/2016 Terms of Use: http://spiedigitallibrary.org/ss/termsofuse.aspx

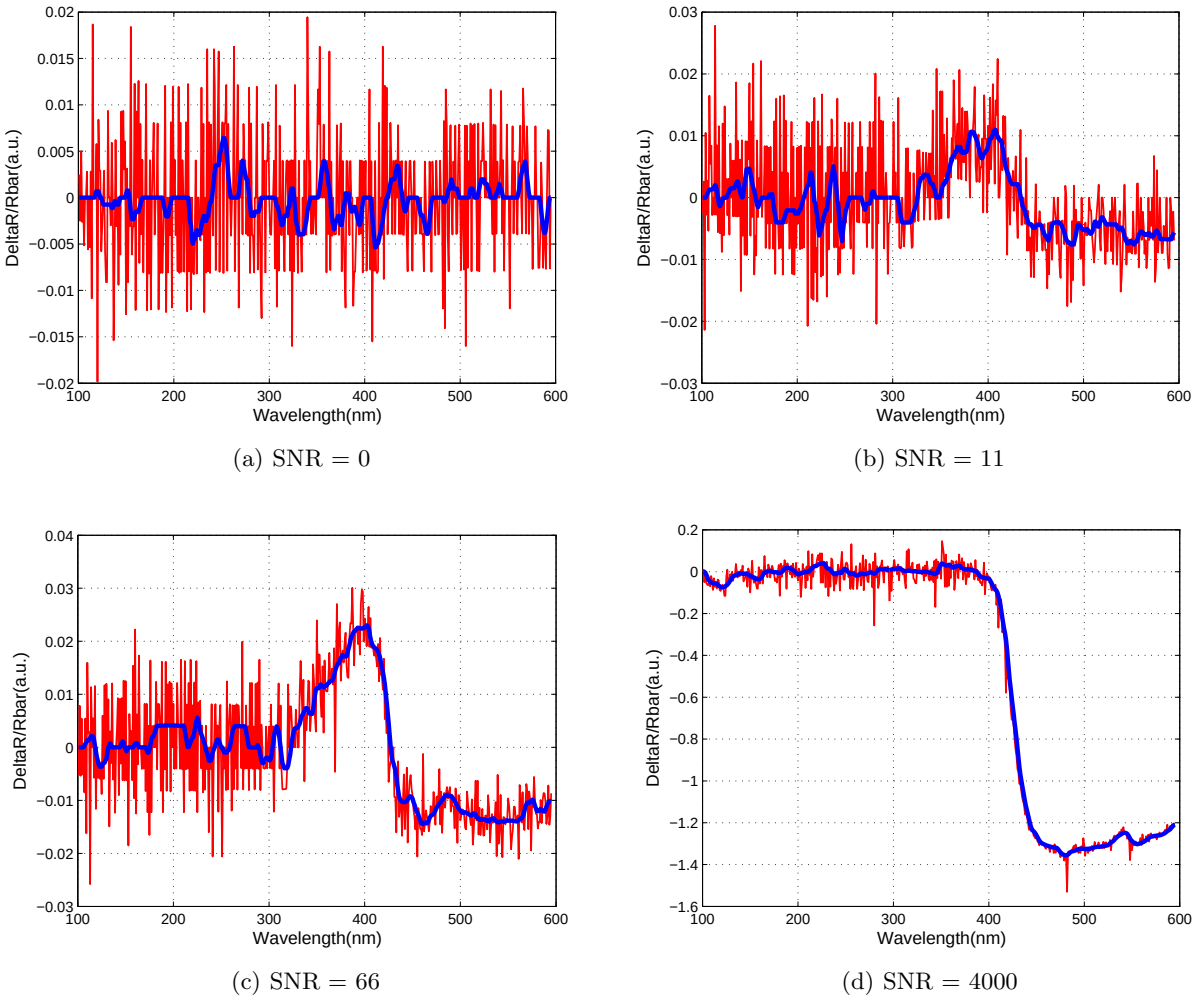

(a) SNR = 0

(b) SNR = 11

(c) SNR = 66

(d) SNR = 4000

Figure 4. TNT signals corresponding to various amounts of TNT. Red is the original signal, and blue is the same spectrum after median and averaging filters. Roughly, the given signal to noise ratio (SNR) values correspond to 400 ng, 2 μg, and 100 μg in (b-d).

[5] Moore, D., "Recent advances in trace explosives detection instrumentation," *Sensing and Imaging: An International Journal* **8**, 9–38 (2007). 10.1007/s11220-007-0029-8.

[6] Moore, D. and Goodpaster, J., "Explosives analysis," *Analytical and Bioanalytical Chemistry* **395**, 245–246 (2009). 10.1007/s00216-009-3003-6.

[7] Hummel, R. E., Fuller, A. M., Schollhrn, C., and Holloway, P. H., "Detection of explosive materials by differential reflection spectroscopy," *Applied Physics Letters* **88**(231903), 898 –910 (2006).

[8] Fuller, A. M., Hummel, R. E., Schoellhorn, C., and Holloway, P. H., "Standoff detection of explosive materials by differential reflection spectroscopy," in [*Proceedings SPIE Optics East*], 2–5 (October 2006).

[9] Hummel, R., Fuller, A., Schoellhorn, C., and Holloway, P., [*Remote Sensing of Explosive Materials using Differential Reflection Spectroscopy*], ch. 15, 301, John Wiley, N.Y. (2007).

[10] Fuller, A. M., *Investigation of select energetic materials by differential reflection spectrometry*, PhD thesis, University of Florida, Department of Materials Science and Engineering (2007).

[11] Schoellhorn, C., Fuller, A. M., Gratier, J., and Hummel, R. E., "New developments on standoff detection of explosive materials by differential reflectometry," in [*SPIE Defense and Security Symposium*], (April 2007).

Downloaded From: http://proceedings.spiedigitallibrary.org/ on 12/25/2016 Terms of Use: http://spiedigitallibrary.org/ss/termsofuse.aspx

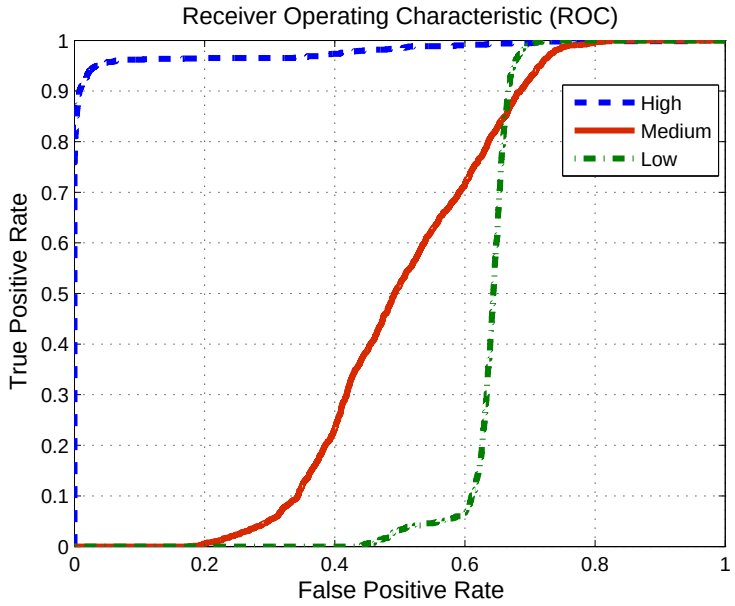

Figure 5. A single SVM classifier was trained on TNT data with high magnitudes, and tested on TNT data with high (blue ROC), medium (red ROC) and low (green ROC) magnitudes of TNT.

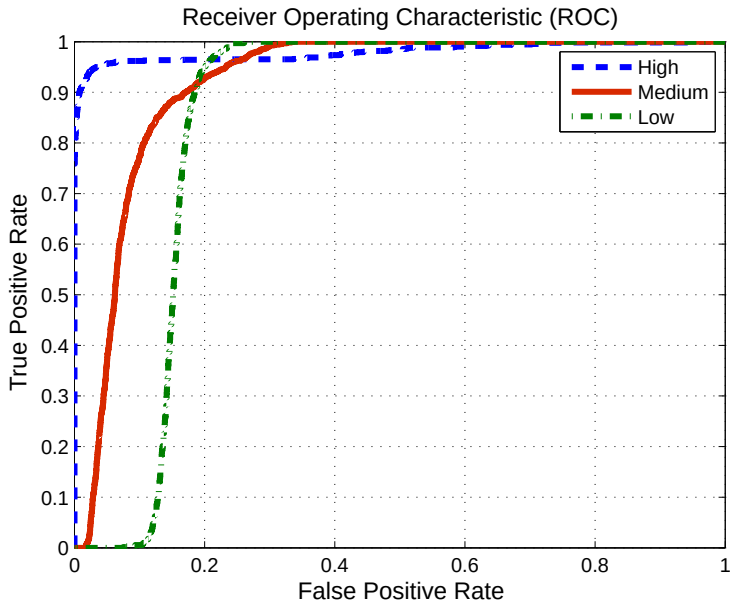

Figure 6. Three SVM classifiers were trained with magnitudes of high, medium and low TNT. The SVM trained on high amounts of TNT were tested against non-TNT signals and TNT signals of high magnitude (blue ROC). Similarly, the SVM trained on medium amounts of TNT were tested against non-TNT signals and TNT spectra with medium magnitudes (red ROC); and the SVM trained on low amounts of TNT were tested against non-TNT signals and TNT spectra with low magnitudes (green ROC).

[12] Schollhorn, C., Fuller, A. M., Gratier, J., and Hummel, R. E., "Developments on standoff detection of explosive materials by differential reflectometry," *Applied Optics* **46**(25), 6232 – 6236 (2007).

[13] Levin, J., Fuller, A., and Hummel, R. E., "Characteristic tnt differential reflection spectra on common

Downloaded From: http://proceedings.spiedigitallibrary.org/ on 12/25/2016 Terms of Use: http://spiedigitallibrary.org/ss/termsofuse.aspx

substances," *Journal of Young Investigators* **1** (July 2009).
[14] Fuller-Tedeschi, A. M. and Hummel, R., "Investigation of the 420 nm differential reflectometry peak for 2,4,6 trinitrotoluene by computational chemistry," *J. Appl. Phys.* **107**(114902), 1–7 (2010).
[15] Dubroca, T., Vishwanathan, K., and Hummel, R. E., "The limit of detection for explosives in spectroscopic differential reflectometry," in [*SPIE Defense and Security Symposium*], (April 2011).
[16] Yuksel, S., Dubroca, T., Hummel, R., and Gader, P., "Spectral analysis for the detection of explosives with differential reflectometry," in [*Grace Hopper Conference (GHC)*], (November 2011).
[17] Zare, A., Gader, P., Bolton, J., Yuksel, S., Dubroca, T., Close, R., and Hummel, R., "Sub-pixel target spectra estimation and detection using functions of multiple instances," in [*IEEE GRSS Workshop on Hyperspectral Image and Signal Processing: Evolution in Remote Sensing (WHISPERS)*], (June 2011).
[18] Vapnik, V. N., [*The nature of statistical learning theory*], Springer-Verlag New York, Inc., New York, NY, USA (1995).
[19] Bishop, C. M., [*Pattern Recognition and Machine Learning (Information Science and Statistics)*], Springer-Verlag New York, Inc., Secaucus, NJ, USA (2006).

Downloaded From: http://proceedings.spiedigitallibrary.org/ on 12/25/2016 Terms of Use: http://spiedigitallibrary.org/ss/termsofuse.aspx